

Article

# Verification of the Ekman Upwelling Criterion with In Situ Temperature Measurements in the Southeastern Baltic Sea

Stanislav Myslenkov <sup>1,2,3,\*</sup> , Ksenia Silvestrova <sup>2</sup> , Viktor Krechik <sup>2</sup> and Mariia Kapustina <sup>2</sup>

<sup>1</sup> Department of Oceanology, Faculty of Geography, Lomonosov Moscow State University, 119991 Moscow, Russia

<sup>2</sup> Shirshov Institute of Oceanology RAS, 117997 Moscow, Russia

<sup>3</sup> Hydrometeorological Research Centre of the Russian Federation, 123242 Moscow, Russia

\* Correspondence: stasocean@gmail.com

**Abstract:** Upwelling leads to a sharp and strong decrease in water temperature in the coastal zone of the southeastern Baltic Sea. The quality of existing hydrodynamic models cannot fully meet the requirements of accurate upwelling forecasts. This study provides insight into the applicability of the simplified Ekman upwelling criterion method for the southeastern Baltic Sea. The upwelling criterion is the ratio of the vertical velocity and the duration of the upwelling wind to the mixed layer density. The vertical velocity was determined by the divergence of the integral Ekman transport in the transverse direction. Calculation of the criterion was based on wind data from NCEP/CFRS reanalysis. The upwelling criterion was compared with in situ temperatures from direct measurements near the D-6 oil platform taken in 2015–2017. Only 46% of calculated upwelling cases were confirmed by temperature decreases in the sub-surface. It was found that more than half of the cases of strong temperature decreases were caused by a northern wind (Ekman upwelling), when the criterion exceeded the threshold value. Comparison of the hydrodynamic model results and direct measurements shows that the model's quality is far from perfect, and the simplified methods can be used as alternatives to models. Some recommendations were made for future upwelling research.

**Keywords:** Baltic Sea; upwelling; upwelling criterion; thermistor chain



**Citation:** Myslenkov, S.; Silvestrova, K.; Krechik, V.; Kapustina, M.

Verification of the Ekman Upwelling Criterion with In Situ Temperature Measurements in the Southeastern Baltic Sea. *J. Mar. Sci. Eng.* **2023**, *11*, 179. <https://doi.org/10.3390/jmse11010179>

Academic Editor: Alfredo L. Aretxabaleta

Received: 13 December 2022

Revised: 30 December 2022

Accepted: 5 January 2023

Published: 10 January 2023



**Copyright:** © 2023 by the authors. Licensee MDPI, Basel, Switzerland. This article is an open access article distributed under the terms and conditions of the Creative Commons Attribution (CC BY) license (<https://creativecommons.org/licenses/by/4.0/>).

## 1. Introduction

In the southeastern coast of the Baltic Sea, one of the most important vertical water exchange mechanisms under the conditions of stable two-layer stratification during the warm period is coastal upwelling [1,2]. This phenomenon occurs mainly under the influence of north, northeast, and east winds [3–5] and has a significant impact on the water column structure, reducing the water temperature in the coastal zone in some cases by more than 8 °C [6,7]. Upwelling's impact on coastal waters and its intensity depends largely on shoreline character and bottom topography [8,9].

Upwelling is one of the most significant factors in nutrient balance in the upper water column [9–11]. In particular, after the first spring phytoplankton bloom, when nutrients in the surface layer are depleted, coastal upwelling is sufficient to sustain the bloom [12].

A large-scale study of the coastal upwelling phenomenon in the Baltic Sea began in the late 1980s when satellite data on sea surface temperature became widely available [13,14]. At present, remote sensing data from infrared radiometers are effectively used to detect and analyze upwelling both in the Baltic Sea and its southeastern part [3,8,15–17]. A total of 135 upwelling events were identified in the southeastern part of the Baltic Sea during the period 2000–2014 (May–October) [2]. Since 2014, there has been an increase in the frequency of upwelling in the southeastern part of the Baltic Sea [18].

However, the regular application of this method is severely limited due to the heavy cloudiness characteristic of some seasons in the Baltic Sea [19]. For this reason, data from satellites equipped with synthetic aperture radars are often used for analysis [19,20]. Less

frequently, field observation data [14,21–25] and mathematical modeling [26–29] are used to study upwelling.

A novel method for studying Baltic Sea coastal upwelling is observations of vertical thermal structure based on the thermistor chain data. Near the Kaliningrad region coast, such a thermistor chain was installed at the D-6 oil platform (LLC LUKOIL KMN) in 2015 [30,31]. Unique for the studied area, this thermistor chain allows for detecting upwelling events and analyzing their occurrence and temporal dynamics [6]. This method of measurement has been successfully applied near the Black Sea coast [32,33]. Much more complete information about the spatiotemporal variability of the water temperature can be obtained by using a cluster of three spaced thermistor chains [34].

A method for calculating the Ekman upwelling criterion based on reanalysis wind data was proposed in [33]. The method is introduced in detail in Section 2.2. Testing this technique on the Black Sea shelf showed good results [35]. When the criterion reached/exceeded a value equal to  $-1$ , a decrease in temperature was observed according to direct measurements. There are a number of works that have used similar methods [36,37]. A similar method of calculating the upwelling index for the area of interest using Ekman transport was used by the authors of [17]. However, the presented calculation was performed without taking into account the thickness of the upper mixed layer, and the water density assumed in the Ekman transport calculations ( $1025 \text{ kg/m}^3$ ) did not correspond to the Baltic Sea's water density.

There are hydrodynamic models that can reproduce such phenomena as upwelling. However, the input data for these models include the initial three-dimensional density fields from climate databases with assimilation of rare CTD profiles. The surface temperature assimilates from satellites 1–2 times every day, but only for the surface layer. Uncertainties in the density field generates baroclinic currents, which in turn interact with wind currents. Thus, modeled data could lead to disagreement with measured data [38]. Therefore, simplified wind schemes are still used for upwelling prediction and analysis in some regions.

In this paper, we present the estimates of the Ekman upwelling criterion for the southeastern Baltic Sea coastal zone. Input data for the calculation include reanalysis wind data and parameters of the water column from direct thermistor chain measurements. The main goal of this study is to calculate the criterion of Ekman coastal upwelling for the area of the Sambia Peninsula and the Curonian Spit coast (Kaliningrad region) and to assess its quality according to in situ measurements.

The paper is organized as follows. We have started with describing the upwelling in the southeastern Baltic Sea. In Section 2, we describe the temperature data and a method for Ekman upwelling calculation. Next, Section 3 presents the main results of the upwelling criterion calculations and verification by thermistor chain data. We consider possible error sources in Section 4. Finally, the conclusion is presented in Section 5.

## 2. Data and Methods

### 2.1. Thermistor Chain Data

The stationary platform D-6 is located approximately 20 km from the shore in the southeastern Baltic Sea (Figure 1). In 2015, a thermistor chain of 10 Starmon mini temperature sensors (produced by Star Oddi, Gardabaer, Iceland) were installed in the middle of the platform's transition bridge [30,31]. The sensors are located on the horizons  $-0.9$  (air), 0.1, 1, 3, 5, 8, 10, 13, 16, 20, 24, and 28 m (Figure 2a). The depth of the site is 29 m. The upper sensor was placed in the air at a height of about 90 cm from the water, and the next sensor was placed 10 cm under the surface. Such sensor distribution provides data for the near-water surface air and the thin upper layer of water in the absence of wind waves. Due to the strong wind waves, the first 4 sensors were placed both in the air and in the water; however, these data can be simply filtered by a sharp increase in temperature dispersion. The time step of temperature measurements is 1 min, the accuracy of sensors is

$\pm 0.025$  °C, and the memory resource in this mode is 480 days. The measurement period that was analyzed in this work ranged from 5 August 2015 to 1 October 2017.

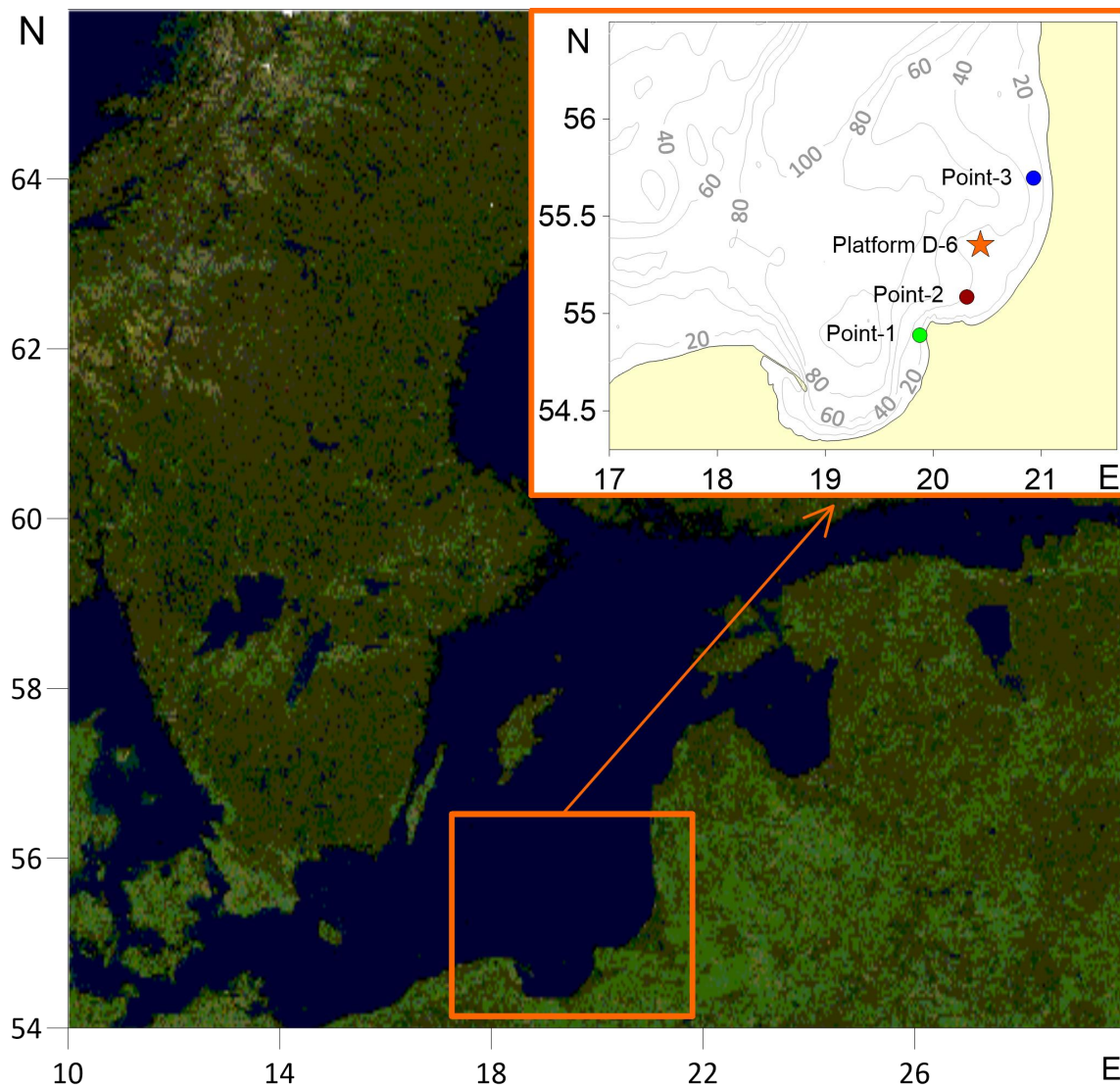


**Figure 1.** Study area, location of oil platform D-6 and points where upwelling criteria are calculated.

The data from the weather station, also installed on the D-6 platform at an altitude of 27 m above sea level, were used as additional information. Air temperature, pressure, wind speed, and direction are available with a time step of 1 h [39].

The mixed layer depth (MLD) was estimated as a depth, where the difference between the surface and the layer water density became more than  $0.125 \text{ kg/m}^3$ . We calculated the daily and monthly averaged MLD. Examples of different MLDs are shown in Figure 2b,c. If the density at the depth increased by more than the criterion of  $0.125 \text{ kg/m}^3$  relative to the surface layer, then the MLD was determined as the closest depth to the criterion (this may be the current depth or the next one). This method is described in [40].

In this area, salinity varies within very small limits (7.1–7.5 in autumn and summer) [41]. In our calculations, we used the uniform salinity value 7.4, which is equal to that observed and analyzed as part of the monitoring values [41,42]. Strong increases in salinity in the bottom layer can occur only with inflows of North Sea waters, which rarely happens [43].

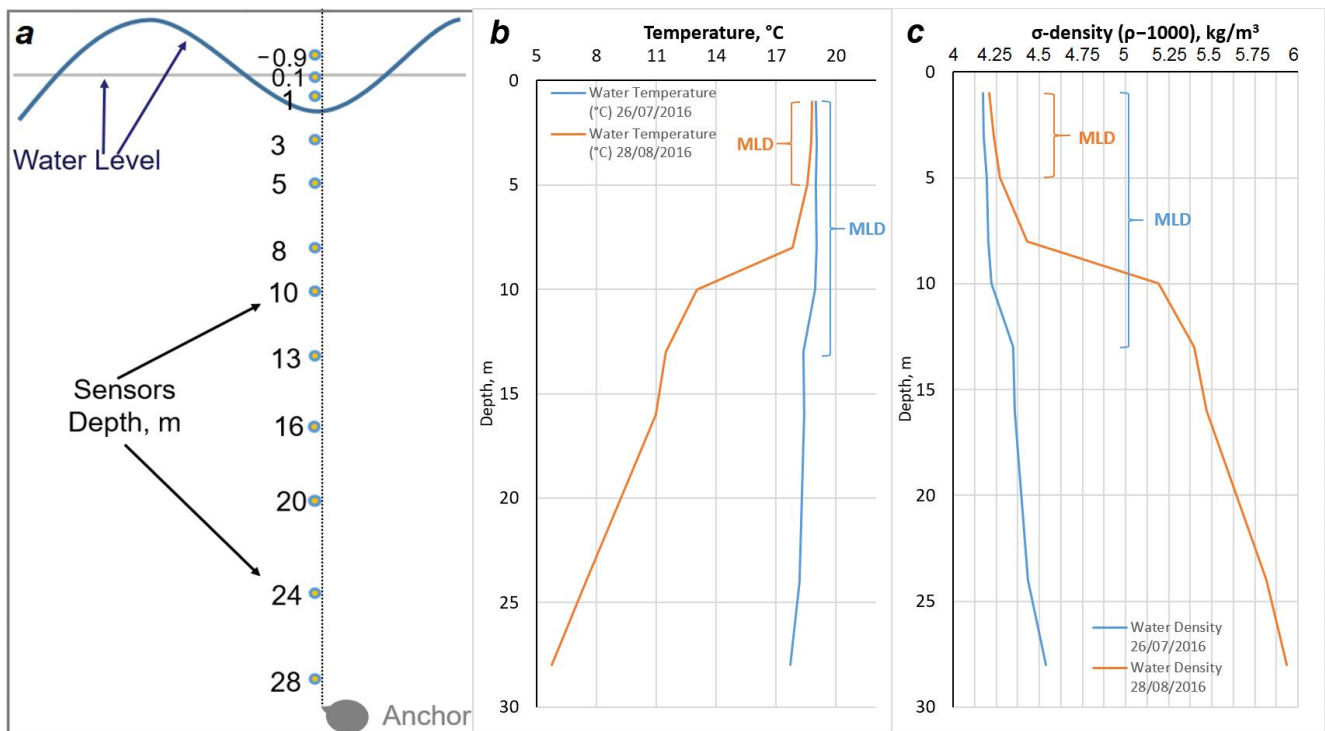


**Figure 2.** The placement of the temperature sensors on the thermistor chain (a). Example of vertical temperature profiles and corresponding MLD (b), vertical density profiles (c) with x-axis spacing of 0.125 kg/m<sup>3</sup>.

### 2.2. Upwelling Criterion Calculation

A special upwelling criterion was applied to assess the possibility of full upwelling due to the wind only (Ekman upwelling), as previously tested in the work [33]. The upwelling criterion is a simple ratio of the vertical velocity ( $w$ ) and the duration of the upwelling wind ( $t$ ) to the MLD ( $H$ ).

$$Ru = w * t/H \tag{1}$$

The vertical velocity is determined by the divergence of the integral Ekman transport in the transverse direction, and the criterion takes the following form:

$$Ru = \tau_y * t/f * \rho_w * H * R_d, \tag{2}$$

where  $\tau_y$  is the alongshore component of the wind stress,  $t$  is the time of the quasi-stationary action of the upwelling wind,  $f$  is the Coriolis parameter,  $\rho_w$  is the density of the seawater,  $H$  is the thickness of the MLD, and  $R_d$  is the local baroclinic radius of Rossby deformation.

This theoretical method (model) assumes that during a strong alongshore wind, the upper layer of water is swept away. The Ekman pumping (proportional to the wind stress and the time of the upwelling wind action) is compared with the MLD. Thus, with their ratio-1 (threshold value of the criterion) subthermocline waters should appear on the surface [33].

A novel step was to provide the real MLD thickness based on in situ data (Section 2.1) as one of the variables in Equation (2), leading to an error in the upwelling estimates. Since the criterion is a cumulative parameter for a certain period of time, we used the MLD before the start of each event.

NCEP/CFSv2 reanalysis data, which have a spatial resolution of  $\sim 0.2^\circ$  and time step of 1 h, were used for wind stress calculation [44].

Additionally, there was an attempt to calculate  $R_d$  from the thermistor chain data (with constant salinity). However, due to the small depth, the thermocline was either absent

or located near the bottom; therefore, the Brunt–Väisälä frequency was small and the  $R_d$  radius was about 0.3–0.5 m. On the other hand, the upwelling criterion implies the use of two-layer stratified water approximation [33]. Therefore, a constant value of  $R_d$  equal to 3.5 km is more acceptable. Such a mean annual value was obtained for the southeastern Baltic Sea near the Gdansk Deep at 60–70 m of depth [45,46], in similar conditions to those near the D-6 platform.

Calculations of the  $R_u$  criterion were carried out for 3 points located in the coastal zone of the Sambia Peninsula (Figure 1). Point 1 is located west of Cape Taran. Point 2 is 5 km north of Zelenogradsk. Point 3 is opposite to the city of Klaipeda (see Figure 2). Ekman upwelling occurs when the alongshore wind blows and removes the top layer of the water. The choice of points provides estimates of the coastal orientation influence. Could upwelling be caused by different winds in the study region? For points 1 and 3, the meridional component of the wind was used for calculating the criterion, and for point 2, the zonal component was used. The criterion was obtained only for the period when the MLD existed (from April to November).

### 2.3. Satellite Data

Multisensory Earth remote sensing data, distributed by the CMEMS (Copernicus Marine Environment Monitoring Service) [47,48], with a spatial resolution of  $0.02 \times 0.02$  degrees, and L3 processing level were used for the additional SST analysis. The data were obtained from different scanners, including AVHRR/3 (MetOp-B, NOAA-18 and NOAA-19), MODIS (Terra and Aqua), VIIRS (Suomi NPP), and AMSR-2 (GCOM-W1). Non-corrected products are 24 hourly syntheses centered at 00 UTC. Quantum-GIS software was used to process and analyze the SST CMEMS data.

### 2.4. Model Data

The CMEMS Baltic Sea Physical Reanalysis [49] data were used for comparison with measured data. This reanalysis was based on the ice–ocean model NEMO-Nordic and provides a daily mean salinity, temperature, horizontal current components, and mixed layer depth with a spatial resolution of 4 km.

## 3. Results

The vertical temperature distribution from the thermistor chain on the D-6 platform was obtained from August 2015 to December 2017. The upwelling criterion was calculated for the same period. For the criterion quality assessments, we used the temperature measurements in the sub-surface and near the bottom. The convective mixing (no vertical stratification) in this region usually begins in September–October, and early stratification is observed in April [30,50]. Therefore, we present the results of the calculation of the criterion and temperature data from 1 April to 1 November, since in the absence of stratification, we are not able to show the vertical movement of water.

The results of  $R_u$  calculations and comparison with the temperature data are presented in Figures 2–5. For points 1 and 3, the wind contributing to the occurrence of Ekman upwelling is northern, and for point 2, eastern. This is due to the orientation of the coastline. According to the theory, when the criterion reaches  $-1$ , cold sub-thermocline waters upwell to the surface [33]. If the criterion is greater than 0, then downwelling should be observed. The criterion is cumulative for a certain period of time, and the mark for each criterion value corresponds to the end of the event (the change in wind direction).

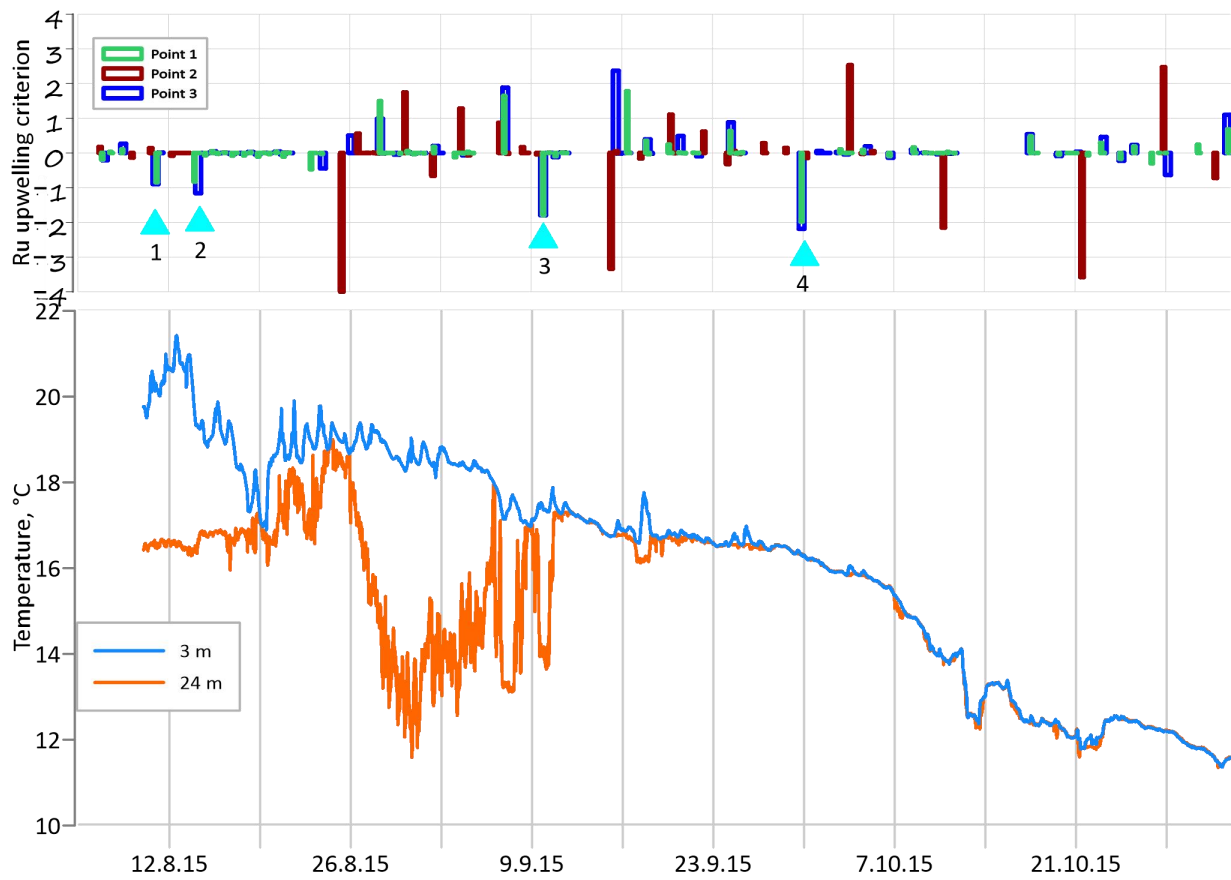


**Figure 3.** Water temperature and upwelling criteria at points 1, 2, and 3 from 5.08.2015 to 1.11.2015. Blue triangles mark upwelling events.

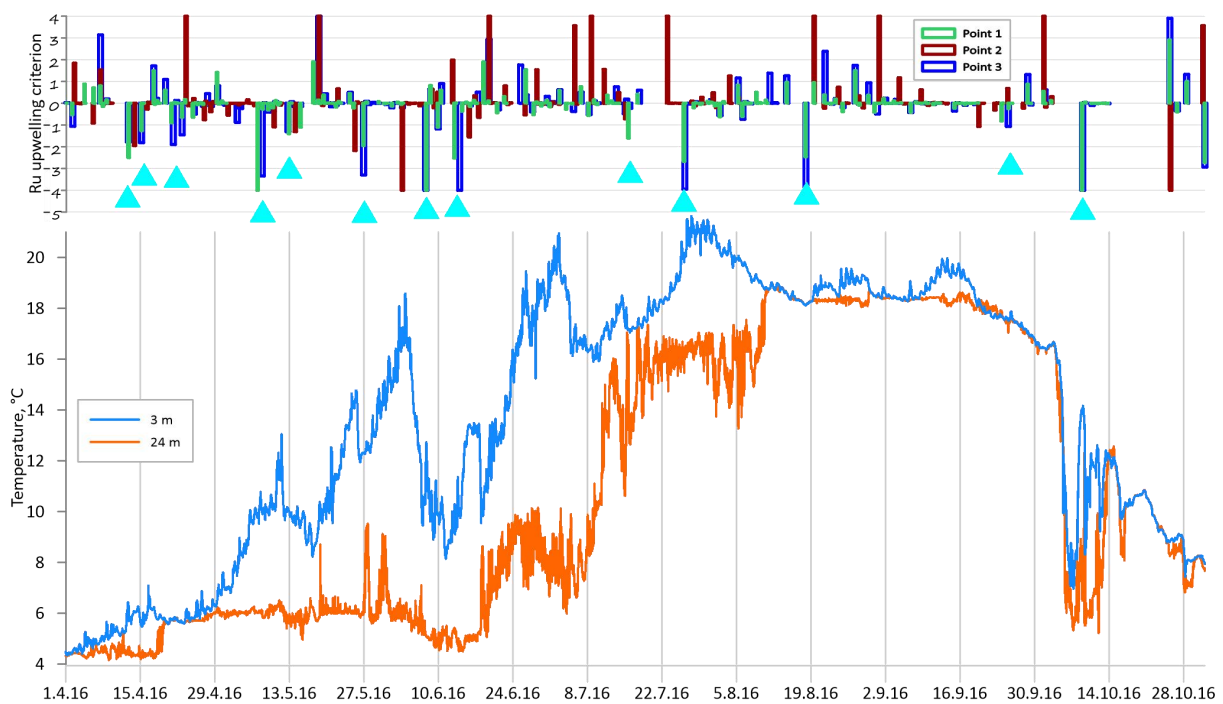


**Figure 4.** Water temperature and upwelling criterion at points 1, 2, and 3 from 1.04.2016 to 1.11.2016. Blue triangles mark upwelling events.

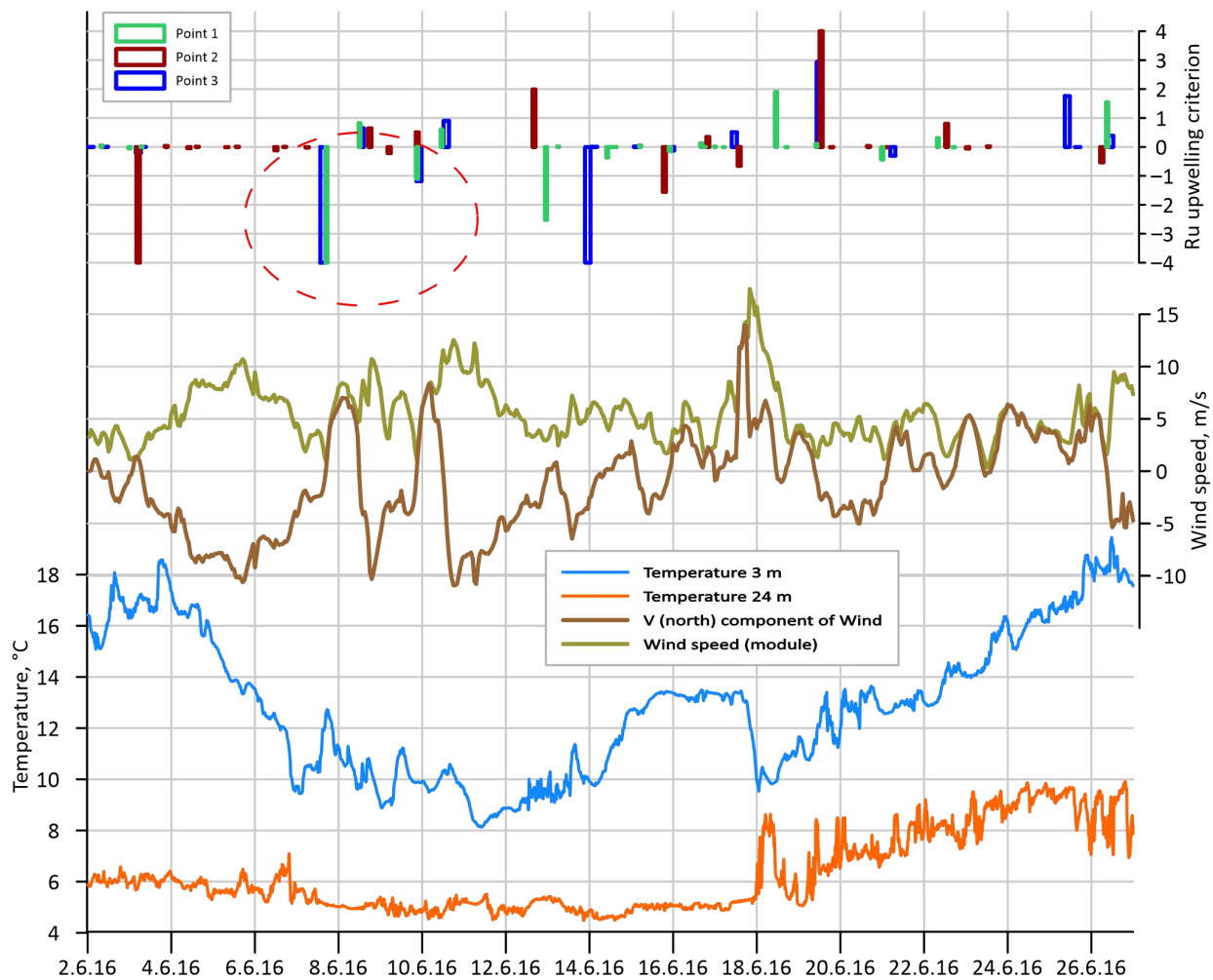


**Figure 5.** Water temperature and upwelling criterion at points 1, 2, and 3 from 2.06.2016 to 26.06.2016. Red circle marks upwelling event.

Figure 3 shows the results of the  $Ru$  calculation for 2015 (August–October). Note that values of the criterion for points 1 and 3 are very similar. Such similarity was caused by the quasi-uniform wind field in our spatial scale (80–100 km). It is evident from Figure 3 that the criterion at point 2 practically does not influence the water temperature. The linear scale of the Sambia Peninsula northern coast is ~30 km, being much smaller than the Curonian and Vistula Spits, with over 150 km. Apparently, the scale of the eastward Sambia coast and general direction of the isobaths near the D-6 platform are unfavorable for the joint upwelling analysis of point 2.

Therefore, we will describe the upwelling cases only for points 1 and 3 as a whole.

We identified four events (blue triangles in Figure 3) when the upwelling criterion reached the value  $-1$ . The first event was recorded on 11 August 2015. The upwelling criterion was  $-0.9$  and temperature decrease was  $0.6\text{ }^{\circ}\text{C}$ . This decrease looks like a diurnal variability rather than upwelling, so the criterion triggered as false. The next event was on 14 August 2015, for which the max  $Ru$  was  $-1.1$  (point 3) and temperature decrease was  $2.3\text{ }^{\circ}\text{C}$ . This case is quite significant, and it considered to be a result of the upwelling. Further, on 17–19 August, we observed a drop in surface temperature from  $19.8$  to  $16.9\text{ }^{\circ}\text{C}$ , which was obviously unrelated to the wind. The third case was observed on 9 September, which showed no change on the surface thermistor, but the temperature near the bottom dropped sharply. Before this case, there were also significant temperature oscillations near the bottom, probably caused by water dynamics/advection. The last case in 2015 was on 29 September, as indicated in Figure 3, but there was no stratification. Thus, we were unable

to estimate vertical water movement. Since convective mixing had already started and there was no stratification, all wind events after 1 October were diluted from the analysis.

Values of the criterion at points 1 and 3 reached +1 due to several downwelling events. For example, the bottom temperature increased to 17.8 °C on 6 September, which seems like a downwelling. However, the main focus of this work was upwelling analysis, so we did not consider downwelling events in detail.

Comparison of the temperature data and the upwelling criterion for 2016 is shown in Figure 4. Vertical thermal stratification in this year started on 10 April and completely disappeared on 20 September due to the autumn cooling and development of convective mixing. During this period, it was possible to identify upwelling events and evaluate the quality of the upwelling criterion. In total, 13 upwelling events were fixed for points 1 and 3 according to the upwelling criterion in 2016. The upwelling criterion for point 2, as in 2015, was weakly related to the temperature changes. For this reason, point 2 events were not considered in the analysis.

According to Figure 4, the upwelling criterion works correctly for several strong events: 13 May, 27 May, and 7 June. The last case in 2016 was observed on 8 October, but the MLD was greater than the depth near the D-6 platform, so we cannot say whether it was upwelling or advection. In other cases, there were no strong temperature drops.

One of the strongest upwelling events during the study period was observed from 5 June to 12 June 2016, as indicated in Figure 5. The cause of the upwelling was a northeastern wind with a speed of ~5–10 m/s from 4 to 7 June (the MLD was 13 m). The upwelling criterion at points 1 and 3 exceeded  $-4$  on 7 June,  $-1$  on 9 June, and  $-4$  again on 12–13 June. The sub-surface temperature dropped from 19 °C to 9 °C and then to 8 °C (Figure 5). According to remote sensing data, a narrow strip of water with a temperature of less than 11 °C was observed along the Curonian Spit on 7 June (Figure 6). However, this phase of low temperatures between 7 and 13 June ought not be considered to be due to wind alone. Apparently, there was an advection of cold waters from the north.

Figure 7 illustrates the upwelling criterion and temperature data for 2017. Altogether, 10 events were identified for points 1 and 3 according to the upwelling criterion calculation in 2017. Upwelling on 10 May and on 3 June was observed in temperature data. For example, the criterion value exceeded the threshold value on 10–11 May at points 1 and 3, and the water temperature decreased from 9 °C to 5 °C. A decrease in temperature (1.8 °C) was observed on 14 June, and the upwelling criterion was  $-1.4$  for point 3. In other cases, small temperature decreases were observed and there was no stratification in the last three cases, so we cannot know the thickness of the MLD, and it is impossible to evaluate the criterion.

According to satellite data from [18], there were 8 upwelling events in 2015, 10 upwelling events in 2016, and 5 upwelling events in 2017 in the area to the north of the Sambia coast and to the west of the Curonian Spit. Some of them we observed by thermistor chain measurements.

After visual analysis, we decided to research statistics of the events. The results are divided into two tables as follows. The first table contains all cases when the calculated upwelling criterion was less than  $-1$ ; the second table contains all events when there was a decrease in sub-surface temperature (2 °C or more). Such a decrease in temperature is considered a strong event (since the amplitude of diurnal variability is less than 1 °C). For statistical analysis, we used those cases when stratification was observed according to the thermistor chain data. If there were less than 2–3 days between events, they were combined into 1 event. Despite the uniformity of the wind field and the similarity of the calculated data, there was some difference between points 1 and 3 and a few cases where the upwelling criterion reached  $-1$  in one of these points.

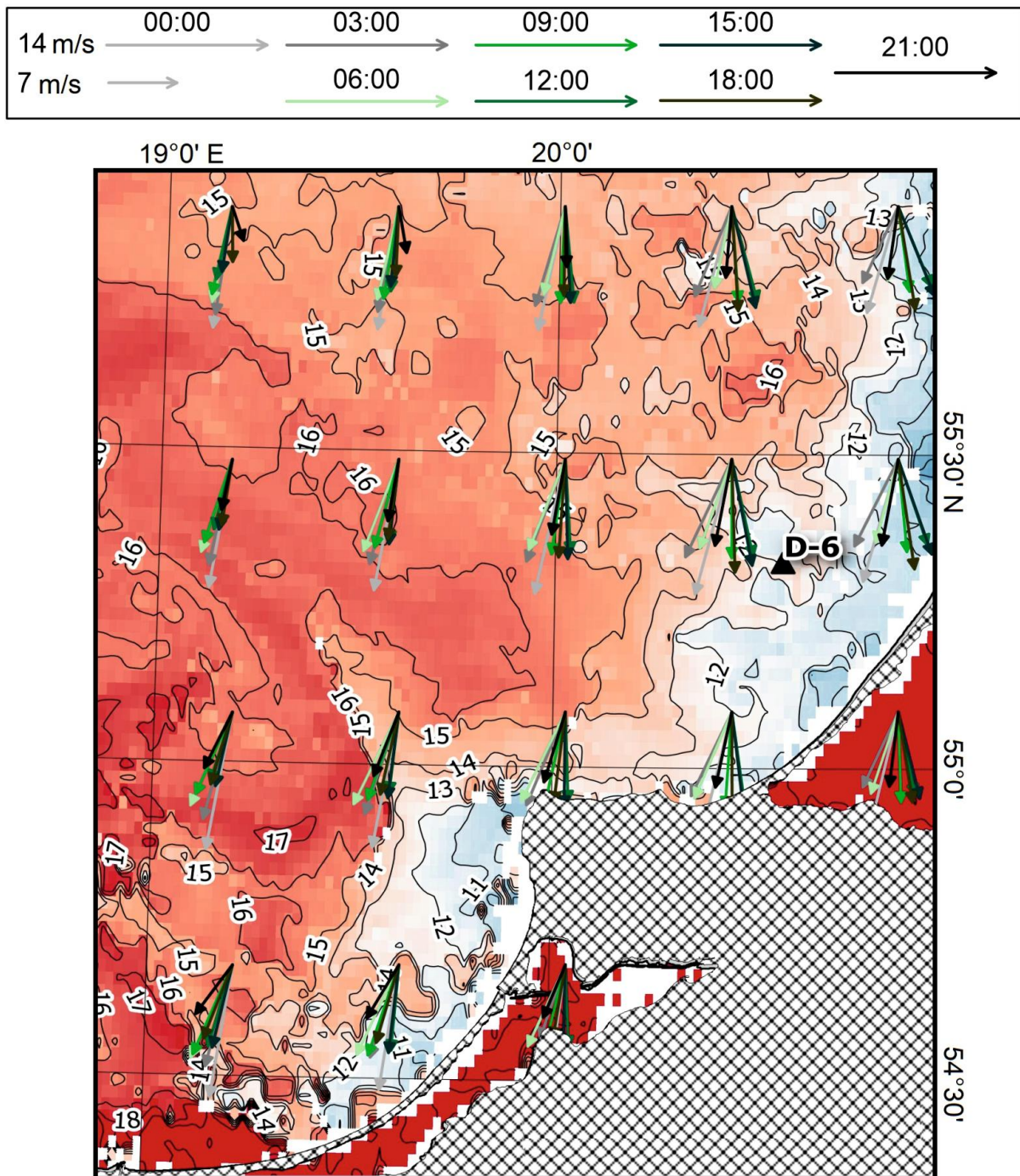


**Figure 6.** Wind speed and direction for 6 June 2016, and surface water temperature according to satellite data for 00:00 on 7 June 2016. Upper panel is a legend for the wind data.

All events for which the calculated upwelling criterion was less than  $-1$  (and vertical stratification was present) are shown in Table 1. It can be clearly seen there was not always a temperature decrease when the upwelling criterion was less than  $-1$ . Only in 33% of events (8 out of 24) did the upwelling criterion work correctly and the temperature drop  $2\text{ }^{\circ}\text{C}$  or more. If we combine good and moderate agreement, then 46% of the calculated events would be included. The main conclusion is that the upwelling criterion is not always reliable in this water area. It should be noted that we were looking only for Ekman upwellings, and did not examine other water dynamics.

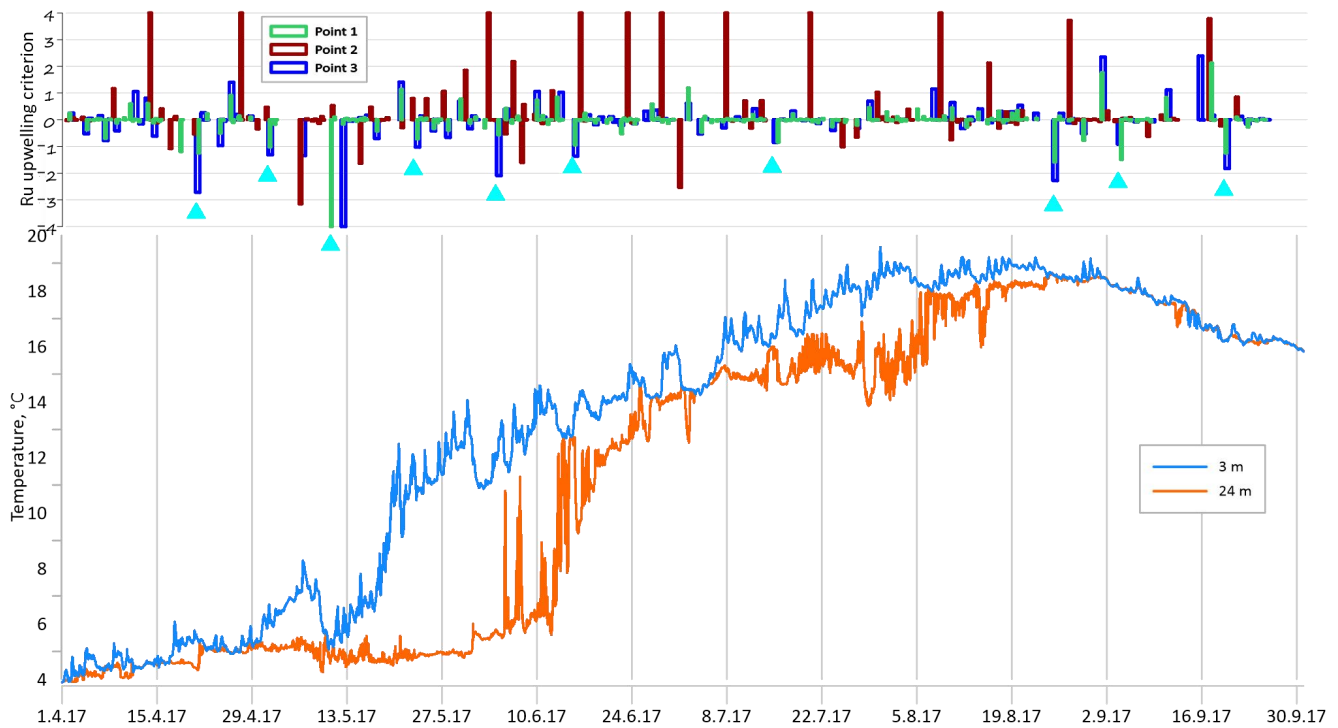


**Figure 7.** Water temperature and upwelling criterion at points 1, 2, and 3 from 1.04.2017 to 1.10.2017. Blue triangles mark upwelling events.

**Table 1.** Events with an upwelling criterion of less than  $-1$  and observed temperature change.

Date	Upwelling Criterion (Point 1/Point 3)	Sub-Surface Temperature Changes (Negative Values Indicate a Decrease), °C	Agreement with Temperature Data	Duration of the Event, Hours (Point 1/Point 3)
11.08.2015	-0.9/-0.9	-0.4	poor	64/60
14.08.2015	-0.1/-1.2	-2.2	good	66/70
09.09.2015	-1.8/-1.8	-0.5	poor	72/70
12.04.2016	-2.5/-1.8	+0.2	bad	99/86
15.04.2016	-1.3/-1.8	-0.7	poor	52/57
20/21.04.2016	-0.9/-1.9	0	poor	28/35
07.05.2016	-4.3/-3.3	+0.6	bad	141/92
12.05.2016	-1.4/-1.3	-3.1	good	40/34
26.05.2016	-1.9/-3.3	-2.6	good	42/60
07.06.2016	-4.5/-6.1	-8.7	good	106/103
12/13.06.2016	-2.6/-5.4	-2.4	good	60/80
15.07.2016	-1.6/-0.5	-1.4	moderate	36/19
26.07.2016	-2.7/-4.0	+2.4	bad	210/204
17.08.2016	-2.5/-4.6	0.0	bad	84/85
25.09.2016	-0.3/-1.1	+0.1	bad	26/137
08.10.2016	-4.1/-4.7	-9.5	good	139/144
20.04.2017	-1.2/-2.7	0.0	bad	52/198
01.05.2017	-1/-1.3	+0.6	bad	68/62
06.05.2017	-/-1.3	-1.4	moderate	see next event/113
10/11.05.2017	-6.6/-7.3	-2.8	good	190/135
22.05.2017	-0.7/-1	-1.5	moderate	57/58
03.06.2017	-0.6/-2.1	-2.7	good	47/78
14.06.2017	-0.9/-1.4	+0.7	bad	45/51
14.07.2017	-0.8/-0.9	-0.2	poor	50/44

Let us consider the results of the evaluation of the upwelling criterion for all events when a temperature drop of 2 degrees or more was observed. All events with a temperature decrease (2 °C or more) in a period of vertical stratification are shown in Table 2. It was found that most events corresponded to a negative upwelling criterion. In 67% (8 out of 12), the upwelling criterion works correctly for the strong drop in temperature. In three cases, the criterion was negative,  $-0.2$ – $-0.4$ , which indicates a favorable wind direction. It could be concluded that more than half of cases had strong connections with water dynamics caused by wind, i.e., a strong temperature decrease often caused by Ekman upwelling in the studied area. Ekman upwelling near the D-6 oil platform is associated with the north wind. However, even if there is a favorable upwelling wind, there could be a dynamic process that prevents the occurrence of upwelling in 54% of cases.

**Table 2.** The events selected based on the temperature decrease (2 °C or more) and calculated upwelling criterion.

Date	Temperature Changes (Negative Values Indicate a Decrease in Temperature)	Upwelling Criterion Point 1/Point 3	Success of the Criterion Work
14.08.2015	−2.2	−0.1/−1.2	moderate
18.08.2015	−2.5	−0.1/−0.04	bad
12.05.2016	−3.1	−1.4/−1.3	good
26.05.2016	−2.6	−1.9/−3.3	good
07.06.2016	−8.7	−4.5/−6.1	good
13.06.2016	−2.4	−2.6/−5.4	good
18.06.2016	−3.4	change in the wind/1.9	bad
05.07.2016	−4.6	−0.1/−0.4	bad
08.10.2016	−9.5	−4.1/−4.7	good
10.05.2017	−2.8	−6.6/−7.3	good
21.05.2017	−3.2	−0.7/−1	good
01.06.2017	−3.0	−0.6/−2.1	good

Due to the unavoidable lack of input data, the calculation method does not always give the correct result. We discuss this in the next section.

For point 2, the upwelling criterion obviously does not work. Since the derivation of the formula for calculating the criterion assumes that the problem is two-dimensional, in order to obtain a correct result, a flat coast of sufficient length is needed (to remove boundary effects). In our case, at point 2, the coast length is about 30 km. The spatial scale of wind upwelling in this area is about 100–150 km (based on the uniformity of the wind field according to reanalysis data). Therefore, the linear scale of the coastline is several times smaller than the scale of the phenomenon.

#### 4. Discussion

In this section, we will consider why the upwelling criterion calculations are not always reliable for the southeastern part of the Baltic Sea.

The quality of the calculated criterion was evaluated only according to the thermistor chain data. The location of the measurement point is at a distance of ~20 km from the coast and ~40–50 km from the nodes of wind reanalysis. So, some errors are possible due to the spatial variability of a temperature and wind field in the research area. However, Figure 6 presents a relatively uniform wind field, and the upwelling is wide. Errors should not be large on such a scale for strong events.

Incorrect values of the Rossby radius and MLD could provide a lot of errors. These values do not affect the sign of the upwelling criterion, but they could change the criterion significantly. For example, if the MLD is set incorrectly, upwelling could either occur at the value of  $-0.5$  or not occur at  $-1.5$ . Unfortunately, the only possible location for the thermistor chain installation had a depth of 28 m. The MLD reaches 40–60 m at this location. It can be assumed that in our case, measurements of the MLD were limited by

location depth. The same problems arise when calculating the Rossby deformation radius. Therefore, an important recommendation for conducting similar studies is to install sensors in a location deeper than the seasonal thermocline depth.

Another important reason for disagreement between the calculated criterion and water temperature is the water dynamics, which are not directly related to the local wind field. According to previous works [17], in some cases, upwelling manifested 4 or more days after favorable wind conditions had been established. In the area of Cape Taran, alongshore currents are often observed to have different directions, as well as various eddies and cyclones recorded by satellite images [51]. The nature of these currents is likely non-local and wind-driven, so the Ekman effects are suppressed and the criterion does not work. Due to the lack of instrumental measurements of the currents and density field, we cannot assert whether there was a baroclinic current against the wind current. It should be stated that measurements of a thermal water structure ought to be accompanied by current measurements (ADCP or at least on several horizons).

The use of this criterion in the Black Sea is more successful, with 70% of calculated cases being determined to be related to a temperature decrease near Gelendzhik [33]. The authors believe that this is due to the weakening of the Main Rim Current in the summer (when the quality of the criterion is evaluated). Weak summer water dynamics encourage manifestations of Ekman upwelling in the coastal zone of the Black Sea. In the Baltic Sea, summer water dynamics are usually stronger; thus, some modification of the research method is necessary—especially for data on currents.

There are various options for using upwelling indexes for the large-scale Eastern boundary upwelling systems [52,53]. These indexes, as well as our method, are based on the wind speed and direction. Large-scale upwelling indexes work well, but in our case, we had a time scale of 1–2 days and a spatial scale of about 100 km, which was probably due to a decrease in method quality.

An obvious question is: is it better to use high-resolution hydrodynamic models where upwelling processes are reproduced? There are well-established models for the Baltic Sea, for example, Baltic Sea Physics Reanalysis from CMEMS [49]. Figure 8 illustrates a comparison of the surface temperature from the model and that from our measurements. Although main seasonal variations in the water temperature are quite similar, it can be clearly seen that the model reproduced only one upwelling event in July correctly (green circle). In other cases (26 May and 07 June), the amplitude of the temperature decrease was half that according to direct measurements. The upwelling with a strong temperature decrease (9.5 °C) on 8 October was not reproduced at all; the upwelling criterion was correct (see Table 2). There is also some artificial temperature variability in the winter due to cloudiness. The near-bottom temperature from the model showed some disagreement with direct measurements during the year.

The above model gaps are caused by the small number of CTD data. The models assimilate the surface temperature only from satellites (1–2 times per day) and the wind from reanalysis. The vertical profile of temperature and salinity is usually climatic with very rare assimilation of soundings. Hence, incorrect baroclinic currents and incorrect MLDs may be present, especially in the coastal zone. Such model limitations lead to the use of simple schemes for wind upwelling research.

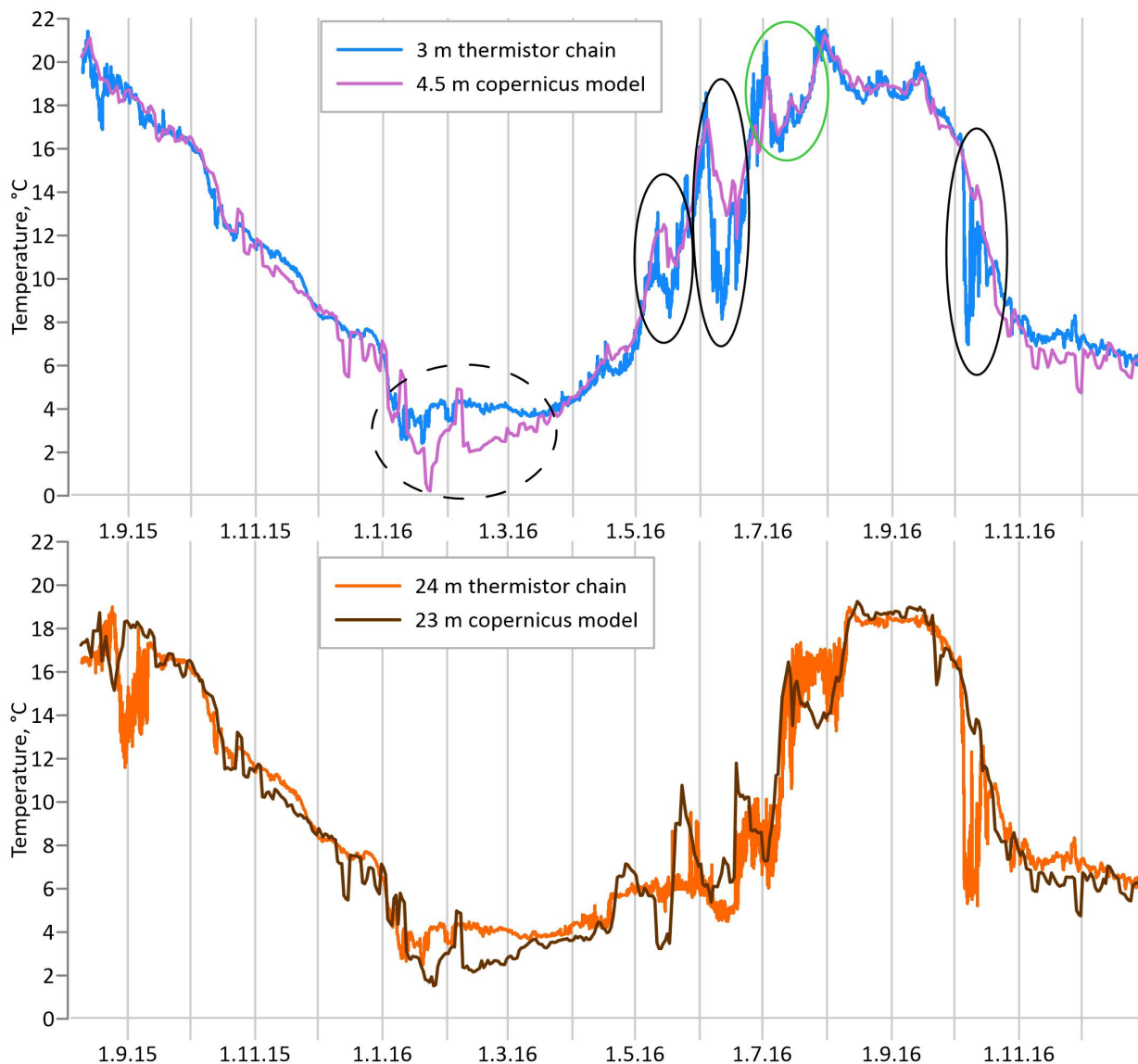


**Figure 8.** Water temperature near the surface and near the bottom according to the thermistor chain and Copernicus model data from 15.08.2015 to 31.12.2016. All solid circles mark upwelling events, and the green circle marks upwelling, as reproduced by the model. Dashed circle marks a winter period, when the model had great discrepancy with measurements.

## 5. Conclusions

This study aimed to assess the applicability of the Ekman upwelling criterion according to thermistor chain data from the southeastern Baltic Sea. The criterion calculation was conducted from August 2015 to November 2017. Input data include wind from reanalysis, MLDs and water temperature from measurements, and constant salinity and Rossby radius from other studies. Results contain a comparison between the calculated criterion and in situ measurements.

It was shown that a temperature decrease ( $2\text{ }^{\circ}\text{C}$  or more) was observed only in 33% of cases when the upwelling criterion was less than  $-1$ . For temperature decreases of more than  $1\text{ }^{\circ}\text{C}$ , we achieved good agreement for 48% of cases with the upwelling criterion. Therefore, it is evident that such a method is unreliable for the studied area.

Nevertheless, 67% of events with strong temperature decreases were connected with an upwelling criterion of less than  $-1$ . Therefore, cold water manifestation near the surface was mostly caused by Ekman upwelling; moreover, it was caused by northern winds.

However, active water dynamics such as baroclinic currents and eddies prevent upwelling and lead to significant errors in Ekman upwelling estimation when using this method. Currents data and baroclinic components should be considered in the method.

Eastern winds did not lead to any decrease in water temperature. Although part of the Sambia Peninsula has a zonal orientation of the coastline, the spatial scale of the Ekman upwelling is larger than 30 km. Several possible reasons for the incorrect operation of the criterion are indicated as follows: location of the measurement point, MLD and Rossby radius instability or wrong calculation of these parameters, and active water dynamics in the studied area, which is not related to the local winds.

Comparison of the model and direct measurements shows that only one case out of four upwellings was reproduced correctly in 2016. The temperature drop was half that shown by direct measurements or there was no drop at all. According to the upwelling criterion, three cases (including some not reproduced by the model) out of the above four were predicted. Due to this fact, simplified methods are still competitive with models in terms of Ekman upwelling studies, as models do not yet give the best results.

To conclude, we will specify useful recommendations for further upwelling research. It is necessary to choose installation depths greater than the seasonal thermocline depth (in the studied area, this would be 60–70 m, for example). It is very useful to install a current meter and salinity sensors together with thermistors. Such sensors will provide correct calculations and more detailed analysis of the upwelling events.

**Author Contributions:** The concept of the study was jointly developed by S.M. and K.S. S.M.: analysis, visualization, and manuscript writing. K.S.: data processing, analysis, writing, and editing. V.K. and M.K. investigation, data processing, analysis, and manuscript writing. All authors have read and agreed to the published version of the manuscript.

**Funding:** Implementation of the upwelling criterion for the Baltic Sea was carried out by Ksenia Silvestrova with the financial support of Grant of the President of the Russian Federation no. MK-709.2021.1.5. Data analysis funded by the Ministry of Science and Higher Education of Russia, theme FMWE-2021-0002. The work of S.A. Myslenkov was supported by the Interdisciplinary Scientific and Educational School of Moscow State University, under “The Future of the Planet and Global Environmental Changes”.

**Institutional Review Board Statement:** Not applicable.

**Informed Consent Statement:** Not applicable.

**Data Availability Statement:** Not applicable.

**Acknowledgments:** Authors are grateful to LLC LUKOIL KMN (Kaliningrad) for their assistance in the installation of equipment and organization of the data acquisition process.

**Conflicts of Interest:** The authors declare no conflict of interest.

## References

1. Kahru, M.; Hakansson, B.; Rud, O. Distribution of the sea-surface temperature fronts in the Baltic Sea derived from satellite imagery. *Cont. Shelf Res.* **1995**, *15*, 663–679. [\[CrossRef\]](#)
2. Esiukova, E.; Chubarenko, I.; Stont, Z. Upwelling or Differential Cooling? Analysis of Satellite SST Images of the Southeastern Baltic Sea. *Water Resour.* **2017**, *44*, 69–77. [\[CrossRef\]](#)
3. Kowalewski, M.; Ostrowski, M. Coastal up-and downwelling in the southern Baltic. *Oceanologia* **2005**, *47*, 435–475.
4. Bednorz, E.; Pótrolniczak, M.; Czernecki, B.; Tomczyk, A.M. Atmospheric forcing of coastal upwelling in the southern Baltic Sea basin. *Atmosphere* **2019**, *10*, 327. [\[CrossRef\]](#)
5. Bednorz, E.; Pótrolniczak, M.; Tomczyk, A.M. Regional circulation patterns inducing coastal upwelling in the Baltic Sea. *Theor. Appl. Climatol.* **2021**, *144*, 905–916. [\[CrossRef\]](#)
6. Krechik, V.; Myslenkov, S.; Kapustina, M. New possibilities in the study of coastal upwellings in the southeastern Baltic sea with using thermistor chain. *Geogr. Environ. Sustain.* **2019**, *12*, 44–61. [\[CrossRef\]](#)
7. Jurkin, V.; Kelpšaitė, L. Upwelling by the Lithuanian coast: Numerical prediction using GIS methods. In Proceedings of the 2012 IEEE/OES Baltic International Symposium (BALTIC), Klaipeda, Lithuania, 2 February 2012; pp. 1–5.
8. Lehmann, A.; Myrberg, K.; Höfllich, K. A statistical approach to coastal upwelling in the Baltic Sea based on the analysis of satellite data for 1990–2009. *Oceanologia* **2012**, *54*, 369–393. [\[CrossRef\]](#)

9. Kowalewski, M. The influence of the hel upwelling (Baltic Sea) on nutrient concentrations and primary production—the results of an ecohydrodynamic model. *Oceanologia* **2005**, *47*, 567–590.
10. Vahtera, E.; Laanemets, J.; Pavelson, J.; Huttunen, M.; Kononen, K. Effect of upwelling on the pelagic environment and bloom-forming cyanobacteria in the western Gulf of Finland, Baltic Sea. *J. Mar. Syst.* **2005**, *58*, 67–82. [[CrossRef](#)]
11. Kuvaldina, N.; Lips, I.; Lips, U.; Liblik, T. The influence of a coastal upwelling event on chlorophyll a and nutrient dynamics in the surface layer of the Gulf of Finland, Baltic Sea. *Hydrobiologia* **2010**, *639*, 221–230. [[CrossRef](#)]
12. Siegel, H.; Gerth, M.; Neumann, T.; Doerffer, R. Case studies on phytoplankton blooms in coastal and open waters of the Baltic Sea using Coastal Zone Color Scanner data. *Int. J. Remote Sens.* **1999**, *20*, 1249–1264. [[CrossRef](#)]
13. Bychkova, I.; Viktorov, S. Use of satellite data for identification and classification of upwelling in the Baltic Sea. *Oceanology* **1987**, *27*, 158–162.
14. Gidhagen, L. Coastal upwelling in the Baltic Sea. Satellite and in situ measurements of sea-surface temperatures indicating coastal upwelling. *Estuar. Coast. Shelf Sci.* **1987**, *24*, 449–462. [[CrossRef](#)]
15. Zhang, S.; Wu, L.; Arnqvist, J.; Hallgren, C.; Rutgersson, A. Mapping coastal upwelling in the Baltic Sea from 2002 to 2020 using remote sensing data. *Int. J. Appl. Earth Obs. Geoinf.* **2022**, *114*, 103061. [[CrossRef](#)]
16. Lehmann, A.; Myrberg, K. Upwelling in the Baltic Sea—A review. *J. Mar. Syst.* **2008**, *74*, S3–S12. [[CrossRef](#)]
17. Dabuleviciene, T.; Kozlov, I.; Vaiciute, D.; Dailidienė, I. Remote sensing of coastal upwelling in the south-eastern Baltic Sea: Statistical properties and implications for the coastal environment. *Remote Sens.* **2018**, *10*, 1752. [[CrossRef](#)]
18. Kapustina, M.V.; Zimin, A.V. Upwelling spatiotemporal characteristics in the southeastern Baltic Sea in 2010–2019. *Fundam. Appl. Hydrophys.* **2021**, *14*, 52–63. (In Russian)
19. Gurova, E.; Lehmann, A.; Ivanov, A. Upwelling dynamics in the Baltic Sea studied by a combined SAR/infrared satellite data and circulation model analysis. *Oceanologia* **2013**, *55*, 687–707. [[CrossRef](#)]
20. Kozlov, I.E.; Kudryavtsev, V.N.; Johannessen, J.A.; Chapron, B.; Dailidienė, I.; Myasoedov, A.G. ASAR Imaging for coastal upwelling in the Baltic sea. *Adv. Space Res.* **2012**, *50*, 1125–1137. [[CrossRef](#)]
21. Krężel, A.; Szymanek, L.; Kozłowski, Ł.; Szymelfenig, M. Influence of coastal upwelling on chlorophyll a concentration in the surface water along the Polish coast of the Baltic Sea. *Oceanologia* **2005**, *47*, 433–452.
22. Krek, A.V.; Krek, E.V.; Danchenkov, A.R.; Krechik, V.A.; Kapustina, M.V. The role of upwellings in the coastal ecosystem of the Southeastern Baltic Sea. *Reg. Stud. Mar. Sci.* **2021**, *44*, 101707. [[CrossRef](#)]
23. Suursaar, U. Combined impact of summer heat waves and coastal upwelling in the Baltic Sea. *Oceanologia* **2020**, *62*, 511–524. [[CrossRef](#)]
24. Ulyanova, M.O.; Sivkov, V.V.; Bashirova, L.D.; Kapustina, M.V.; Bubnova, E.S.; Danchenkov, A.R.; Ezhova, E.E.; Krechik, V.A.; Eremina, T.R. Oceanological Research of the Baltic Sea in the 51st Cruise of the PV Akademik Sergey Vavilov (June–July 2021). *Oceanology* **2022**, *62*, 578–580. [[CrossRef](#)]
25. Sivkov, V.V.; Ulyanova, M.O.; Kapistina, M.V.; Bubnova, E.S.; Dorokhov, D.V.; Krechik, V.A.; Dudkov, I.Y.; Dvoeglazova, N.V. Integrated Research of the Southern Part of the Baltic Sea in the 49th Cruise of the Akademik Sergey Vavilov. *Oceanology* **2020**, *60*, 567–569. [[CrossRef](#)]
26. Kowalewska-Kalkowska, H.; Kowalewski, M. Combining Satellite Imagery and Numerical Modelling to Study the Occurrence of Warm Upwellings in the Southern Baltic Sea in Winter. *Remote Sens.* **2019**, *11*, 2982. [[CrossRef](#)]
27. Golenko, N.N.; Golenko, M.N.; Shchuka, S.A. Observation and modeling of upwelling in the southeastern Baltic. *Oceanology* **2009**, *49*, 15–21. [[CrossRef](#)]
28. Nowicki, A.; Janecki, M.; Dzierzbicka-Głowacka, L. Operational system for automatic coastal upwelling detection in the Baltic Sea based on the 3D CEMBS model. *J. Oper. Oceanogr.* **2019**, *12*, 104–115. [[CrossRef](#)]
29. Stepanova, N.; Mizyuk, A. Tracking the formation of the gradient part of the southeastern Baltic Sea cold intermediate layer. *Russ. J. Earth Sci.* **2020**, *20*, ES3005. [[CrossRef](#)]
30. Myslenkov, S.A.; Krechik, V.A.; Bondar, A.V. Daily and seasonal water temperature changes in the coastal zone of the Baltic Sea measured by thermistor chain. *Ecol. Syst. Devices.* **2017**, *5*, 25–33, (In Russian with English summary).
31. Myslenkov, S.A.; Krechik, V.A.; Soloviev, D.M. Water temperature analysis in the coastal zone of the Baltic Sea based on thermistor chain observations and satellite data. *Proc. Hydrometcentre Russ.* **2017**, *364*, 159–169, (In Russian with English summary).
32. Ocherednik, V.; Baranov, V.; Zatsepin, A.; Kyklev, S. Thermochains of the Southern Branch, Shirshov Institute of Oceanology, Russian Academy of Sciences: Design, Methods, and Results of Metrological Investigations of Sensors. *Oceanology* **2018**, *58*, 661–671. [[CrossRef](#)]
33. Silvestrova, K.P.; Zatsepin, A.G.; Myslenkov, S.A. Coastal upwelling in the Gelendzhik area of the Black Sea: Effect of wind and dynamics. *Oceanology* **2017**, *57*, 469–477. [[CrossRef](#)]
34. Ocherednik, V.V.; Zatsepin, A.G.; Kuklev, S.B.; Baranov, V.I.; Mashura, V.V. Examples of approaches to studying the temperature variability of black sea shelf waters with a cluster of temperature sensor chains. *Oceanology* **2020**, *60*, 149–160. [[CrossRef](#)]
35. Silvestrova, K.; Myslenkov, S.; Zatsepin, A. Variability of Wind-Driven Coastal Upwelling in the North-Eastern Black Sea in 1979–2016 According to NCEP/CFSR Data. *Pure Appl. Geophys.* **2018**, *175*, 4007–4015. [[CrossRef](#)]
36. Bakun, A. *Coastal Upwelling Indices, West Coast of North America, 1946–1971*; U.S. Department of Commerce NOAA Technical Report NMFS-SSRF: Seattle, WA, USA, 1973; pp. 1–103.

37. Gonzalez-Nuevo, G.; Gago, J.; Cabanas, J.M. Upwelling index: A powerful tool for marine research in the NW Iberian upwelling system. *J. Oper. Oceanogr.* **2014**, *7*, 47–57. [CrossRef]
38. BALTICSEA\_REANALYSIS\_PHY\_003\_011//Quality. Information Document.—2019. —P. 4. 5. Available online: <https://catalogue.marine.copernicus.eu/documents/QUID/CMEMS-BAL-QUID-003-011.pdf> (accessed on 10 December 2022).
39. Stont, Z.I.; Bukanova, T.V. General features of air temperature over coastal waters of the south-eastern Baltic Sea for 2004–2017. *Russ. J. Earth. Sci.* **2019**, *19*, ES3001. [CrossRef]
40. Monterey, G.; Levitus, S. Seasonal Variability of Mixed Layer Depth for the World Ocean. In *NOAA Atlas NESDIS*; National Oceanic and Atmospheric Administration: Silver Spring, MD, USA, 1997; Volume 14, p. 100.
41. Kapustina, M.V.; Krechik, V.A.; Gritsenko, V.A. Seasonal variations in the vertical structure of temperature and salinity fields in the shallow Baltic Sea off the Kaliningrad Region coast. *Russ. J. Earth. Sci.* **2017**, *17*, ES1004. [CrossRef]
42. Sivkov, V.V.; Kadzhoyan, Y.S.; Pichuzhkina, O.Y.; Feldman, V.N. *Oil and Environment of the Kaliningrad Region*; Terra Baltika: Kaliningrad, Russia, 2012. (In Russian)
43. Demidov, A.N.; Koltovskaya, E.V.; Kulikov, M.E. Long-term changes of thermohaline characteristics of the Baltic Sea. *Vestn. Mosk. Univ. Seriya 5 Geogr.* **2018**, *4*, 49–56. (In Russian)
44. Saha, S.; Moorthi, S.; Wu, X.; Wang, J.; Nadiga, S.; Tripp, P.; Behringer, D.; Hou, Y.T.; Chuang, H.Y.; Iredell, M.; et al. The NCEP Climate Forecast System version 2. *J. Clim.* **2014**, *27*, 2185–2208. [CrossRef]
45. Osinski, R.; Rak, D.; Walczowski, W.; Jan, P. Baroclinic Rossby radius of deformation in the southern Baltic Sea. *Oceanologia* **2010**, *52*, 417–429. [CrossRef]
46. Kurkin, A.; Kurkina, O.; Rybin, A.; Talipova, T. Comparative analysis of the first baroclinic Rossby radius in the Baltic, Black, Okhotsk, and Mediterranean seas. *Russ. J. Earth Sci.* **2020**, *20*, ES4008. [CrossRef]
47. CMEMS Baltic Sea the DMI Sea Surface Temperature Reprocessed L3S. Available online: <https://doi.org/10.48670/moi-00312> (accessed on 10 December 2022). [CrossRef]
48. Høyer, J.L.; Le Borgne, P.; Eastwood, S. A bias correction method for Arctic satellite sea surface temperature observations. *Remote Sens. Environ.* **2014**, *146*, 201–213. [CrossRef]
49. CMEMS: Baltic Sea Physics Reanalysis, CMEMS [Data Set]. 2022. Available online: <https://doi.org/10.48670/moi-00013> (accessed on 10 December 2022). [CrossRef]
50. Stepanova, N.B.; Shchuka, S.A.; Chubarenko, I.P. Structure and evolution of the cold intermediate layer in the southeastern part of the Baltic Sea by the field measurement data of 2004–2008. *Oceanology* **2015**, *55*, 25–35. [CrossRef]
51. Leppäranta, M.; Myrberg, K. *Physical Oceanography of the Baltic Sea*; Springer, Praxis Publishing: Chichester, UK, 2008; p. 370.
52. Abrahams, A.; Schlegel, R.W.; Smit, A.J. Albertus Variation and Change of Upwelling Dynamics Detected in the World’s Eastern Boundary Upwelling Systems. *Front. Mar. Sci.* **2021**, *8*, 626411. [CrossRef]
53. Bonino, G.; Di Lorenzo, E.; Masina, S.; Iovino, D. Interannual to decadal variability within and across the major Eastern Boundary Upwelling Systems. *Sci. Rep.* **2019**, *9*, 19949. [CrossRef]

**Disclaimer/Publisher’s Note:** The statements, opinions and data contained in all publications are solely those of the individual author(s) and contributor(s) and not of MDPI and/or the editor(s). MDPI and/or the editor(s) disclaim responsibility for any injury to people or property resulting from any ideas, methods, instructions or products referred to in the content.